The Kinetic Pathway of Folding of Barnase

ARTICLE *in* JOURNAL OF MOLECULAR BIOLOGY · NOVEMBER 2003

Impact Factor: 4.33 · DOI: 10.1016/j.jmb.2003.08.024 · Source: PubMed

doi:10.1016/j.jmb.2003.08.024 J. Mol. Biol. (2003) 333, 169–186

JMB

Available online at www.sciencedirect.com

SCIENCE DIRECT®

ELSEVIER

The Kinetic Pathway of Folding of Barnase

Faaizah Khan, Jessica I. Chuang, Stefano Gianni and Alan R. Fersht*

MRC Centre for Protein Engineering, MRC Centre Hills Road, Cambridge CB2 2QH, UK

To search for folding intermediates, we have examined the folding and unfolding kinetics of wild-type barnase and four representative mutants under a wide range of conditions that span two-state and multi-state kinetics. The choice of mutants and conditions provided in-built controls for artifacts that might distort the interpretation of kinetics, such as the non-linearity of kinetic and equilibrium data with concentration of denaturant. We measured unfolding rate constants over a complete range of denaturant concentration by using by $^{1}H/^{2}H$-exchange kinetics under conditions that favour folding, conventional stopped-flow methods at higher denaturant concentrations and continuous flow. Under conditions that favour multi-state kinetics, plots of the rate constants for unfolding against denaturant concentration fitted quantitatively to the equation for three-state kinetics, with a sigmoid component for a change of rate determining step, as did the refolding kinetics. The position of the transition state on the reaction pathway, as measured by solvent exposure (the Tanford β value) also moved with denaturant concentration, fitting quantitatively to the same equations with a change of rate determining step. The sigmoid behaviour disappeared under conditions that favoured two-state kinetics. Those data combined with direct structural observations and simulation support a minimal reaction pathway for the folding of barnase that involves two detectable folding intermediates. The first intermediate, I_1, is the denatured state under physiological conditions, D_{Phys}, which has native-like topology, is lower in energy than the random-flight denatured state U and is suggested by molecular dynamics simulation of unfolding to be on-pathway. The second intermediate, I_2, is high energy, and is proven by the change in rate determining step in the unfolding kinetics to be on-pathway. The change in rate determining step in unfolding with structure or environment reflects the change in partitioning of this intermediate to products or starting materials.

*Corresponding author

Keywords: intermediates; protein; folding; NMR; mechanism

Introduction

One of the most vexing areas in mechanistic studies is the question of intermediates: do they exist and are they on-pathway? A reaction that fits simple two-state kinetics or fits a single exponential may hide a high-energy intermediate that is kinetically silent. A reaction that fits multi-state kinetics or multiple exponential phases may be a two-state reaction with complications from off-pathway steps. There are three criteria in classical mechanistic chemistry for a particular molecule to be considered an on-pathway intermediate, the intermediate must be isolated and characterized; it must be formed fast enough to be on the reaction pathway; and it must react fast enough.[1] This "proof" of an on-pathway intermediate relies on the intermediate being stable and not rearranging during its isolation. Unfortunately, intermediates in rapid protein folding kinetics are usually conformationally mobile and are exceptionally difficult to isolate or characterize, and so the problem of intermediates is especially fraught for studies of protein folding.

A different approach has to be applied to intermediates in protein folding studies: infer from kinetics that an intermediate is formed, use kinetic criteria to show that it is on pathway and then characterize it if possible by a technique such as

Abbreviations used: I_1, first intermediate; GdmCl, guanidine hydrochloride.

E-mail address of the corresponding author: arf25@cam.ac.uk

Φ-value analysis.[2,3,4] Unfortunately, protein folding is very subject to artifacts, such as reversible aggregation of the denatured state, that gives rise to kinetics that looks like that from a genuine intermediate. Also, some proteins form metastable, misfolded states that are off-pathway but give rise to similar kinetics to that for on-pathway, and other proteins may do the same under forcing conditions.[1] These complications have been discovered in recent years and so require earlier work to be re-examined in the light of new information. The Englander school[5] has re-evaluated much earlier work and has concluded that most, if not all, of the early work that proposes intermediates is incorrect and that all protein folding is two-state, as found for CI2.[6] In contrast, Sanchez & Kiefhaber have re-examined many proteins that are proposed to be two-state and have concluded that all, with CI2 being a notable exception, are multi-state.[7,8]

The 110-residue protein barnase has been extensively studied as a paradigm for multi-state folding[3] and there is a wealth of independent evidence in favour of an on-pathway intermediate, summarized by Fersht.[9] Nevertheless, Bai and co-workers have disputed the very existence of the barnase folding intermediate.[10,11,12] For example, a kinetic test first applied to detect an intermediate in barnase folding, "rollover" (downward curvature) in chevron plots[4] was suggested to result from the movement of transition state ensemble with denaturant concentration in folding and unfolding studies. Fersht[9] argued that the downward curvature in the dependence of the unfolding kinetics of barnase has to result from a change in rate-determining step with denaturant concentration, and hence implies an intermediate, because the curvature is too sharp to come from a gradual movement of the structures of transition states and ground states with concentration of denaturant. The unfolding kinetics fits quantitatively to equations for a change in rate determining step. Similarly, Sanchez & Kiefhaber consider that the urea-dependence of the folding and unfolding of barnase fits quantitatively to a scheme with two intermediates and not to a long gradual movement of the transition state.[8]

Kinks in unfolding kinetics that may be attributed to a change in rate determining step provide a very powerful test for the presence of on-pathway folding intermediates.[9,13,14,15] This is especially so if comparative kinetics can be performed on mutants of the protein that can change the apparent kinetics of folding and unfolding. In this study, we analyse in depth the unfolding kinetics of wild-type barnase and several mutants. Unfolding under conditions that favour folding was measured by $^{1}H/^{2}H$-exchange kinetics, and unfolding at higher denaturant concentrations by conventional stopped-flow methods. We chose representative mutants that have been shown in previous studies to exhibit different types of behaviour regarding two-state and multi-state kinetics. These mutants acted as internal controls from their comparative behaviour. N58A has kinetics that is closer to two-state, as has S91A.[16] 85–102 (cross-linked by Cys85 and Cys102) has extreme deviation from two-state.[17] 43–80 (cross-linked by Cys43 and Cys80) has a closing rate constant in $^{1}H/^{2}H$-exchange that is higher than that expected from its folding rate constant, strongly indicative of a folding intermediate.[18] The mutants affect the mechanism of folding in different ways. NMR experiments on the denatured state[19,20] and peptides[21] show that there is residual structure in the β-hairpin that encompasses residues 85–102. Φ-value analysis implies that the hairpin initiates folding. According to our interpretation of all previous experiments, the mutation S91A raises the energy of the first transition state of folding, whereas cross-linking 85–102 should stabilize that hairpin, and hence the folding intermediate. The mutation N58A deletes a bond that stabilizes the native structure, and not the folding intermediate. Cross-linking 43–80 puts an unnatural constraint into the denatured state.[22,23] We also varied conditions, from those that favour multi-state kinetics for wild-type (pH 6–7, temperature $<30\,^{\circ}C$) to those where the kinetics tend to approach two-state (pH >7.6, temperature $>30\,^{\circ}C$).

We found in the present study that under conditions that favour two-state folding for wild-type protein and for mutants that fold by approximately two-state kinetics, there was a smooth change of unfolding rate constant with concentration of denaturant. However, under conditions previously found to favour multi-state folding, the unfolding kinetics fitted quantitatively to kinetic equations for a three-state pathway with curvature. We could also plot the movement of the transition-state along the reaction co-ordinate and note the change from formation to breakdown with increasing concentrations of GdmCl. Thus, we confirmed conclusively that barnase has an on-pathway folding intermediate. Further, this intermediate is additional to the early intermediate first detected,[3] and is presumably the one detected in simulation[24] and postulated in earlier kinetic studies.[25]

Results

Conventional stopped-flow kinetics of folding and unfolding

Chevron plots

The logarithms of rate constants for folding (k_f) and unfolding (k_u) were plotted against [GdmCl] to generate conventional chevron plots (Figure 1). Plots for wild-type and mutants had a small downward curvature in plots of $\log k_u$ *versus* [GdmCl], as previously noted for the unfolding of wild-type barnase and its mutants in solutions of urea where there are excellent fits to a second-order polynomial.[26] Under conditions where barnase has been proposed to fold *via* multi-state kinetics,[27] the

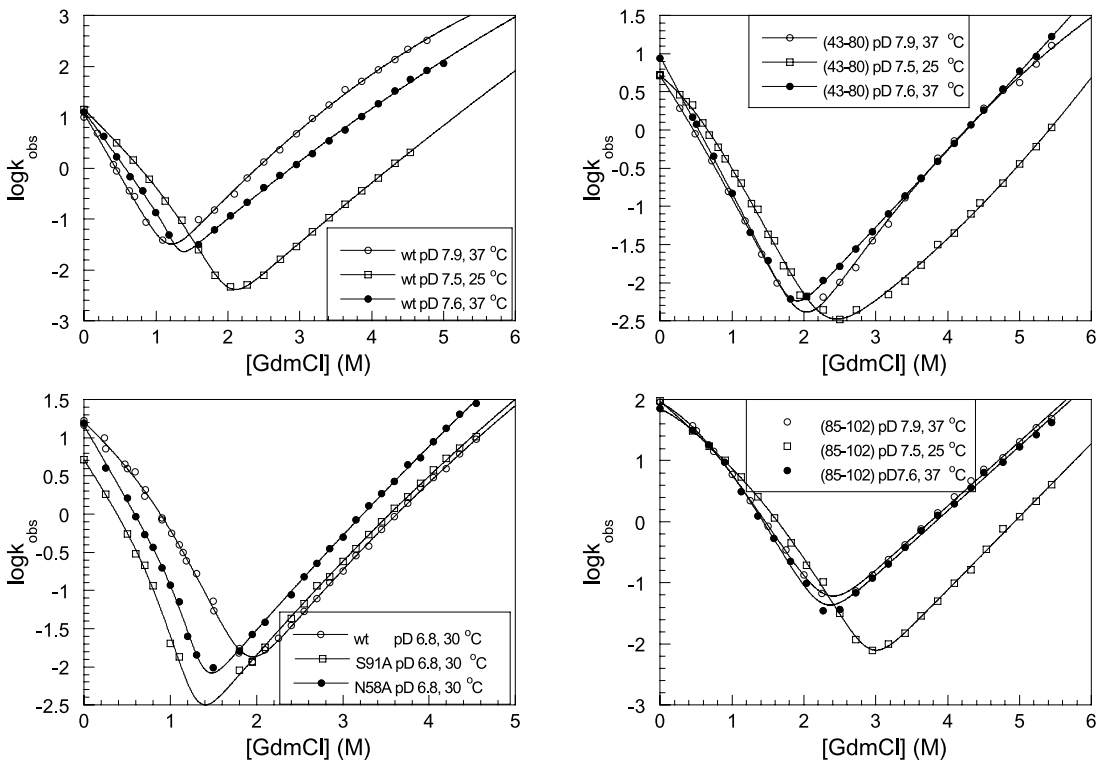

Figure 1. Denaturant dependence of the folding and unfolding kinetics (chevron plots) of wild-type barnase (wt) and mutants 43–80, S91A, N58A and 85–102 at conditions indicated in the Figure. The continuous line represents the best fit of each data set to equation (8).

refolding limb of some of the plots of $\log k_f$ *versus* [GdmCl] also had downward curvature that varied markedly according to the mutant, the pH and temperature, similar to that observed previously in the presence of urea.[3,28] Under conditions that were previously postulated to favour two-state kinetics, the curvature disappeared and there were some striking linear plots.

Kinetic analysis

Data were, accordingly, fitted to the minimal scheme for three-state kinetics (equation (1)):

$$\mathrm{D} \underset{k_{-1}}{\overset{k_1}{\rightleftarrows}} \mathrm{I} \underset{k_{-2}}{\overset{k_2}{\rightleftarrows}} \mathrm{N} \tag{1}$$

or to a simple two-state scheme, where appropriate. The following equations were used, assuming that only the $\log k_{-2}$ term showed a significant non-linear dependence on [GdmCl]. Even if that assumption is wrong, it should not lead to serious error, since the curvature is apparent only at high concentrations of GdmCl, over which $\log k_{-2}$ is measured, and the other rate constants are studied at low concentrations of GdmCl where deviations from a second-order term would not be so apparent:

$$\log k_1 = \log k_1^{\mathrm{H_2O}} - m_1[\mathrm{GdmCl}] \tag{2}$$

$$\log k_{-1} = \log k_{-1}^{\mathrm{H_2O}} + m_{-1}[\mathrm{GdmCl}] \tag{3}$$

$$\log k_2 = \log k_2^{\mathrm{H_2O}} - m_2[\mathrm{GdmCl}] \tag{4}$$

$$\log k_{-2} = \log k_{-2}^{\mathrm{H_2O}} + m_{-2}[\mathrm{GdmCl}] - m_{-3}[\mathrm{GdmCl}]^2 \tag{5}$$

In theory, the kinetics of formation of N should be fitted to the two roots of a quadratic equation.[9] In practice, there are too many variables, especially, as only one of the two relaxations time is observed. Two approximations are generally used in such situations. One extreme is that the intermediate is assumed to be in the steady state at a low concentration, when $k_1 > k_2$. The rate constant is then: $k_f = k_1k_2/(k_2 + k_{-1})$. There are again too many variables to fit the dependence of k_{obs} on [GdmCl], but the solution is simplified by recasting in the form:

$$k_f = k_1/(1 + k_{-1}/k_2) \tag{6}$$

where k_{-1}/k_2 is the partition ratio for the intermediate reverting to starting materials rather than products. The curvature is then due to a change in rate determining step because of the differential effect of GdmCl concentration on k_{-1} and k_2, i.e. its partitioning ratio. The other extreme approximation is that of a rapid pre-equilibrium intermediate when $k_1 > k_2$ and k_{-1}, and $k_{-1} > k_2$. Under such conditions:

$$k_f = k_2/(1 + k_{-1}/k_1) \tag{7}$$

the curvature in this case is due to a decrease in the

Table 1. Kinetic constants of barnase and its mutants that fit three-state kinetics

Protein	Temperature (°C, pH)	$k_0^{H_2O}$ (s^{-1})	$k_{-2}^{H_2O}$ (s^{-1})	m_0 (M^{-1})	m_{-2} (M^{-1})	m_{-3} (M^{-2})	K	m_p (M^{-1})
Wild-type	25, p^2H 7.5	14.6(±0.8)	$5.1(\pm2.5)\times10^{-6}$	1.4(±0.1)	1.3(±0.1)	0.02(±0.01)	30(±20)	1.3(±0.1)
	30, p^2H 6.8	17.2(±1.0)	$1.6(\pm0.6)\times10^{-5}$	1.4(±0.05)	1.6(±0.2)	0.07(±0.02)	14(±8)	1.37(±0.07)
85–102	25, p^2H 7.5	96.6(±7.7)	$7.9(\pm9.6)\times10^{-7}$	1.0(±0.1)	1.3(±0.2)	0.01(±0.02)	50(±25)	1.01(±0.06)
	37, p^2H 7.6	134(±12)	$7.0(\pm2.6)\times10^{-6}$	0.0(±0.3)	1.66(±0.07)	0.07(±0.01)	2(±0.4)	1.7(±0.3)
	37, p^2H 7.9	83(±10)	$5.2(\pm3.6)\times10^{-6}$	0.3(±0.3)	1.7(±0.2)	0.08(±0.02)	6(±2)	1.6(±0.2)
43–80	25, p^2H 7.5	6.7(±0.7)	$1.9(\pm1.2)\times10^{-4}$	0.5(±0.2)	0.2(±0.1)	0.08(±0.01)	3(±1)	1.3(±0.2)
S91A	30, p^2H 6.8	5.2(±0.4)	$2.3(\pm0.8)\times10^{-5}$	1.96(±0.08)	1.50(±0.09)	0.06(±0.02)	50(±75)	2.1(±0.4)
N58A	30, p^2H 6.8	14(±1)	$6(\pm2)\times10^{-5}$	1.9(±0.1)	1.4(±0.1)	0.04(±0.01)	1500(±3000)	2.8(±0.5)

Data were fitted to equation (8), where the constants are defined. The mean and standard error for all the constants were calculated from the curve fitting by the Kaleidagraph program.

concentration of the intermediate with increasing [GdmCl]. I accumulates at low-[GdmCl] and so its breakdown is rate determining. At high-[GdmCl], either the formation or a combination of formation and partitioning of I is rate determining. Equations (6) and (7) are identical in form and one cannot distinguish between the two possibilities *a priori* without additional information.[29]

The data in Figure 1 for the proteins with curved refolding limbs were fitted to:

$$\log k_{obs} = \log (k_0^{H_2O}10 \wedge (-m_0[G])/(1 + K10 \wedge (m_K[G])) + k_{-2}^{H_2O}10 \wedge (m_{-2}[G] - m_{-3}[G]^2)) \quad (8)$$

where k_{obs} is the observed rate constant for folding or unfolding at a particular concentration of GdmCl, abbreviated to G, k_0 could be k_1 or k_2, and K is either k_{-1}/k_2 or k_{-1}/k_1, respectively (for equations (6) and (7), Table 1). The value of k_0 is given with precision from the equation, but K is determined with any degree of reliability only when there is marked curvature in the plot of $\log k_f$ *versus* [GdmCl].

Wild-type barnase refolded at p^2H 6.8 and 30 °C, and at p^2H 7.5 and 25 °C with distinctly downward curvature (Figure 1) and fitted three-state kinetics (Table 1). The values of K were somewhat imprecise. The kinetics became two-state at higher temperature and p^2H (Figure 1; Table 2). The mutant 85–102 showed deviation from two-state kinetics at all conditions of temperature and p^2H (Figure 1; Table 1); 43–80 approached two-state kinetics under the same conditions (Figure 1). S91A and N58A at p^2H 6.8 and 30 °C fitted weakly to three-state kinetics, with values of K that had standard errors greater than the mean (Figure 1; Table 1), but had discernible curvature in the refolding limb.

There were some indications that the mutant 43–80 had an additional fast phase in the kinetics, just discernible at 37 °C and pH 7.6 and 7.9 (data not shown). On excitation at 280 nm and collecting emission at greater than 320 nm, the amplitude of the fastest phase was 5% of that of the major phase in the absence of denaturant. The rate constant for the fastest phase at pH 7.6 was 24 s^{-1}, and that for the major phase 5.5 s^{-1}. At pH 7.9, they were 20 and 4.9 s^{-1}, respectively. However, we consider that the small amplitudes are not conclusive evidence of real phases.

Sub-millisecond mixing experiments

On pH-jumping freshly denatured wild-type barnase from pH 1.5 to pH 7.5 and 25 °C using a continuous flow spectrofluorimeter[30] with excitation at 280 nm and emission at 330(±25) nm, we found a rapid decrease of fluorescence with rate constant 8000 s^{-1} (Figure 2). The amplitude of this phase was about 10% of that of the major refolding phase, but of the opposite sign. On diluting denatured barnase in 2.5 M GdmCl at pH 7.5 to a final concentration of 0.23 M GdmCl, there was a small increase in fluorescence of rate

Table 2. Kinetic constants of barnase and its mutants that fit two-state kinetics

Protein	Temperature (°C, pH)	$k_1^{H_2O}$ (s^{-1})	$k_{-1}^{H_2O}$ (s^{-1})	m_1 (M^{-1})	m_{-1} (M^{-1})	m_{-2} (M^{-2})
Wt	37, p^2H 7.6	14.5(±1.2)	$2.1(\pm0.7)\times10^{-4}$	2.1(±0.05)	1.44(±0.1)	0.05(±0.01)
Wt	37, p^2H 7.9	11.4(±1.0)	$1.96(\pm0.7)\times10^{-4}$	2.4(±0.06)	1.8(±0.1)	0.09(±0.01)
43–80	37, p^2H 7.6	9.8(±0.5)	$3.3(\pm0.9)\times10^{-5}$	1.8(±0.02)	1.1(±0.06)	0.01(±0.01)
43–80	37, p^2H 7.9	5.7(±0.4)	$1.3(\pm0.6)\times10^{-6}$	1.7(±0.03)	1.8(±0.1)	0.09(±0.01)

Data fitted to two-state kinetics where the refolding limb follows: $\log k_1 = \log k_1^{H_2O} - m_1[\text{Gdmcl}]$ and the unfolding: $\log k_{-1} = \log k_{-1}^{H_2O} + m_{-1}[\text{Gdmcl}] - m_{-2}[\text{Gdmcl}]^2$. The mean and standard error for all the constants were calculated from the curve fitting by the Kaleidagraph program.

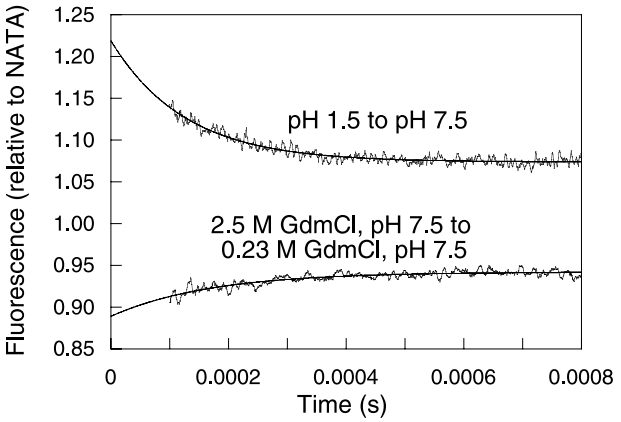

Figure 2. Continuous-flow kinetic traces for the initial steps in the refolding of denatured wild-type barnase on either a pH-jump to pH 7.5 or a dilution of GdmCl. The fluorescence emission relative to that of a standard solution of *N*-acetyltryptophanamide (NATA) is plotted *versus* time.

constant 6000 s^{-1} and amplitude about 3% of that of the major phase (Figure 2). The decrease in fluorescence on acid jump is significantly above any level of artifacts. The small increase is just at the level of detection.

Opening/unfolding kinetics from H/^{2}H-exchange and unfolding profiles

Values of rate constants in equation (1) can be obtained by combining rate constants for unfolding, measured by conventional stopped-flow kinetics at concentrations of denaturant that favour unfolding with measurements of hydrogen-exchange of globally exchanging protons by NMR under conditions that favour folding.[9]

The rate constant for exchange, k_{ex}, for three-state folding where exchange:

$$\text{exchange} \overset{k_{int}}{\leftarrow} \text{D} \underset{k_{-1}}{\overset{k_1}{\rightleftarrows}} \text{I} \underset{k_{-2}}{\overset{k_2}{\rightleftarrows}} \text{N} \qquad (9)$$

takes place only from D and not I (equation (9)) is given at low concentrations of GdmCl[9] by:

$$k_{ex} = \frac{k_{int}\dfrac{k_{-1}k_{-2}}{k_2 + k_{-1}}}{k_{int} + \dfrac{k_1 k_2}{k_2 + k_{-1}}} \qquad (10)$$

where k_{int} is the intrinsic rate constant for exchange under the reaction conditions†. Equation (10) is analogous to the classical equation for exchange,[31] $k_{ex} = k_{int}k_o(k_{int} + k_c)$, where the "closing" rate constant $k_c = k_1k_2/(k_2 + k_{-1})$, and the "opening" $k_o = k_{-1}k_{-2}/(k_2 + k_{-1})$. The measurements under the EX1 limit ($k_{int} \gg k_c$) and in the region of the changeover to EX2 ($k_{int} \sim k_c$) allows both k_o and k_c to be obtained. As described for the derivation of equation (6):

$$k_o = k_{-2}/(k_2/k_{-1} + 1) \qquad (11)$$

The data for the unfolding limb of the chevron plots and the values of k_o were combined to give plots against [GdmCl] (Figure 3; Table 3). The combined data were fitted to equation (12):

$$\log k_{obs} = \log k_{-2}^{H_2O} + m_{-2}[G] - m_{-3}[G]^2 - \log((k_2/k_{-1})10 \wedge (-m_K[G]) + 1) \qquad (12)$$

where m_K is the *m*-value for k_2/k_{-1}, as described.[9]

The term k_2/k_{-1} is the partitioning of the intermediate, between folding to N and reversion to D. At pH 6.8 and 30 °C, there was strong curvature in the plot for wild-type with $k_2/k_{-1} = 36 \pm 8$, a strong commitment to folding. It is always possible that non-linearity in the relationship between the denaturation activity of GdmCl can lead to artifacts at low concentrations because of its effects on ionic strength or that curvature could result from other unknown artifacts. S91A and N58A provided excellent controls for the previously noted distinct curvature in the plot for wild-type (Figure 3). N58A has a very low curvature at low ionic strength and that of S91A is also very small, strongly implying that the curvature in the wild-type plot is real (Figure 3). N58A fitted equation (12) with a commitment of $k_2/k_{-1} = 1.6 \pm 0.8$, and S91A fitted with 2.8 ± 0.4.

The logarithms of the commitment factors for wild-type and the two mutants at 30 °C decreased with *m*-values of 1.3–1.8 with [GdmCl] which caused the rate-determining transition state for unfolding to move from being predominantly that for k_{-1} at low-[GdmCl] to k_{-2} at high-[GdmCl]. The high commitment factor for wild-type led to a very marked change in the plot of unfolding rate *versus* [GdmCl], the low ones for SA91 and NA58, to shallow changes. The low commitment factors of SA91 and NA58 were consistent with the weak fit to a three-state mechanism for the folding kinetics.

The change in partitioning of unfolding of wild-type is also seen as the conditions were varied (Figure 3). At 25 °C and pH 7.5, $k_2/k_{-1} = 100 \pm 70$, and its sensitivity to denaturant of 1.8 M^{-1} was similar to that at pH 6.8 and 30 °C. At 37 °C and pH 7.6, the plot was much smoother and the partitioning dropped to 15 ± 5. At 37 °C and pH 7.9, the unfolding curve gave just a smooth fit to second-order exponential. The commitment to folding of 85–102 at 37 °C and pH 7.6 was also low, at 2.5 ± 1, and the fit to the equation was no better than to a simple second-order exponential without a change of rate determining step (Figure 3). The plot for 43–80 was more noticeably curved (Figure 3).

† http://www.fccc.edu/research/labs/roder/sphere

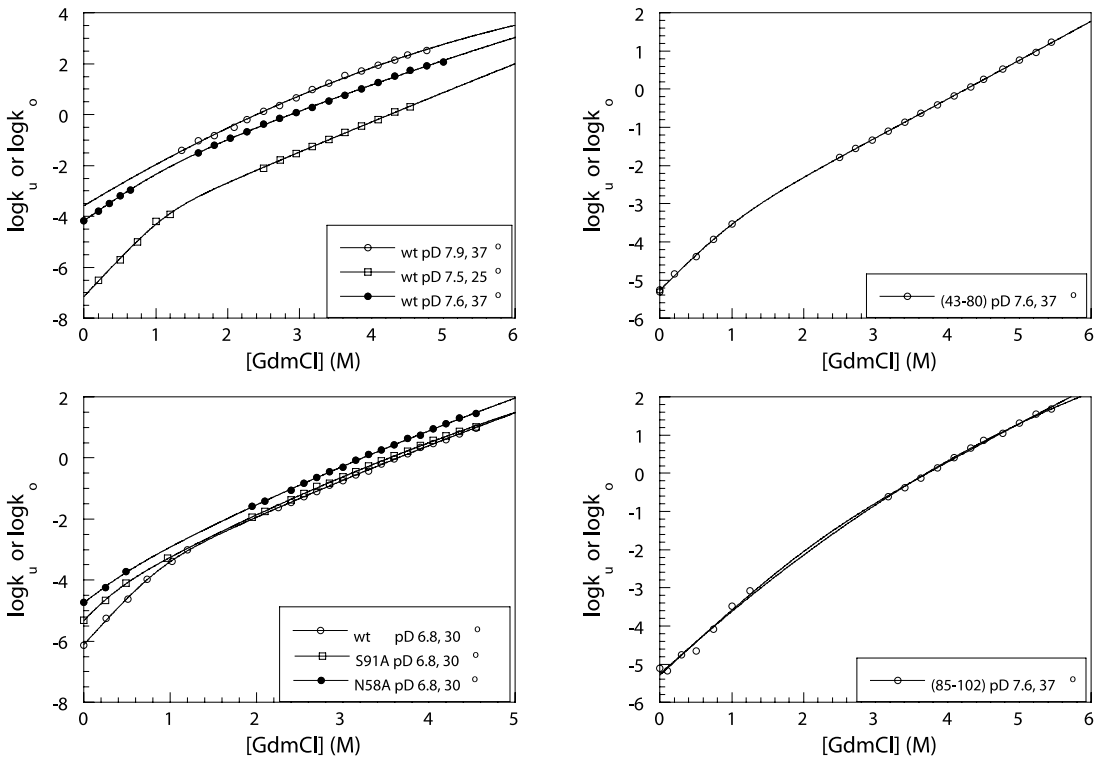

Figure 3. Plots of log k_o and log k_u *versus* GdmCl concentration for wild-type barnase (wt) and mutants 43–80, S91A, N58A and 85–102 at conditions indicated in the Figure. The continuous line represents the best fit of each data set to equation (12) and in the case of 85–102 the fit to a simple second-order polynomial is also shown.

Closing kinetics from $^1H/^2H$-exchange

The exchange of the protons that require global unfolding is very slow in the absence of denaturant, which affected the choice of experimental conditions. 85–102 and 43–80 were, accordingly, studied at higher pH and higher temperatures for the best accuracy (37 °C, > pH 7.6). The half-life in water for globally exchanging protons varied from 2×10^5–10^4 seconds for 43–80 and from 2×10^6 to 2×10^5 seconds for 85–102. Wild-type protein was readily studied at 30 °C and above. At 25 °C and pH 7.5, the slowest exchange rates were at the limit of detection in water, with half-lives of 10^7 seconds. The rate constants were very sensitive to the concentration of GdmCl, and the half-lives decreased dramatically. Reactions were monitored for up to five to seven days, over which period the proteins were stable. Rate constants were determined either by initial rates for the very slowest exchanging protons in water or, more generally, from the full first-order decay curves for the faster exchanging protons in water and for all protons in the presence of moderate concentrations of GdmCl.

The rate of folding decreases and the rate of unfolding increases with increasing [GdmCl]. Accordingly, as the concentration of GdmCl increases, the mechanism of exchange for the protons that require global unfolding should tend to the EX1 limit, with the rate constant for each proton being the same as that for global unfolding, and independent of the value of k_{int}. This is readily seen in Figure 4, where the rate constants at 0.5 M, 0.75 M and 1.0 M GdmCl for 43–80 at pH 7.7 and 37 °C are virtually independent of the value of k_{int}. But, there is a noticeable increase in k_{ex} with increasing k_{int} at 0 M GdmCl. Values of k_{ex} at 0 M GdmCl against k_{int} for 43–80 fitted adequately to a Michaelis–Menten type saturation curve at 0 M GdmCl (duplicate runs at pH 7.7 plus data from Perrett *et al.*[18]) showing that the mechanism was changing from EX2 to EX1 with increasing k_{int}.

The calculation of k_o from the equation $k_{ex} = k_{int}k_o/(k_{int} + k_c)$ is independent of the value of k_{int}, but the derived value of k_c depends directly on the value of k_{int}. It was noted previously that the use of standard values of k_{int} (derived from web), based on values given by Bai *et al.*[32] give values of k_c that are a factor of two to three times lower than expected from accurately measured values of refolding rate constants under appropriate conditions, k_c cannot be lower than the refolding rate constant. We confirmed this discrepancy in the present study under our reaction conditions and used a conversion factor of 2.5 to increase the tabulated values of k_{int}. For example, using a factor of 2.5 at pH 6.8 and 30 °C, the refolding rate constant in the absence of denaturant for S91A was 5.19 s^{-1} and $k_c = 5.2 \pm 1\ s^{-1}$, for N58A it was 15.2 s^{-1} and $k_c = 15.2 \pm 2\ s^{-1}$, and for wild-type it was 15.8 s^{-1} and $k_c = 12 \pm 2\ s^{-1}$. There was similarly good agreement at low concentrations of denaturant for

Table 3. Unfolding and opening constants

Protein	Temperature (°C, p²H)	k_{-2} (s^{-1})	$m_{k_{-2}}$ (M^{-1})	$m^2_{k_{-2}}$ (M^{-2})	k_2/k_{-1}	m_{k_{-1}/k_2} (M^{-1})	k_c (s^{-1})[a]	k_o (s^{-1})[b]
Wild-type	25, 7.5	$7.4(\pm 4) \times 10^{-6}$	$1.25(\pm 0.2)$	$0.01(\pm 0.03)$	$103(\pm 70)$	$1.8(\pm 0.1)$	$13.5(\pm 3.5)$	$7.7(\pm 1.2) \times 10^{-8}$
	30, 6.8	$2.9(\pm 0.6) \times 10^{-5}$	$1.4(\pm 0.06)$	$0.03(\pm 0.01)$	$36(\pm 8)$	$1.8(\pm 0.06)$	$15(\pm 8)$	$8.2(\pm 1.0) \times 10^{-7}$
	37, 7.6	$1.1(\pm 0.4) \times 10^{-3}$	$1.2(\pm 0.1)$	$0(\pm 0.01)$	$15(\pm 5 \times 10^{-5}$	$0.98(\pm 0.05)$	$14.6(\pm 2.6)$	$6.9(\pm 0.4) \times 10^{-5}$
85–102	37, 7.6	$1.1(\pm 0.1) \times 10^{-5}$	$1.6(\pm 0.05)$	$0.06(\pm 0.01)$	$2.5(\pm 0.9)$	$1.0(\pm 0.2)$	$360(\pm 90)$	$5.4(\pm 0.6) \times 10^{-6}$
43-80	37, 7.6	$5.4(\pm 0.7) \times 10^{-5}$	$1.0(\pm 0.1)$	$0.0(\pm 0.0)$	$9.0(\pm 2.9)$	$1.02(\pm 0.04)$	$36(\pm 6)$	$5.5(\pm 0.4) \times 10^{-7}$
S91A	30, 6.8	$1.8(\pm 0.1) \times 10^{-5}$	$1.6(\pm 0.03)$	$0.06(\pm 0.01)$	$2.8(\pm 1.0)$	$1.9(\pm 0.2)$	$2.0(\pm 1.1)$	$4.9(\pm 0.4) \times 10^{-6}$
N58A	30, 6.8	$4.7(\pm 0.6) \times 10^{-5}$	$1.5(\pm 0.1)$	$0.05(\pm 0.01)$	$1.6(\pm 0.8)$	$1.3(\pm 0.3)$	$15.1(\pm 0.2)$	$1.8(\pm 0.06) \times 10^{-5}$

[a] From fits of log k_c *versus* [GdmCl].
[b] From fits of log k_o *versus* [GdmCl] at low-[GdmCl]. The mean and standard error for all the constants were calculated from the curve fitting by the Kaleidagraph program.

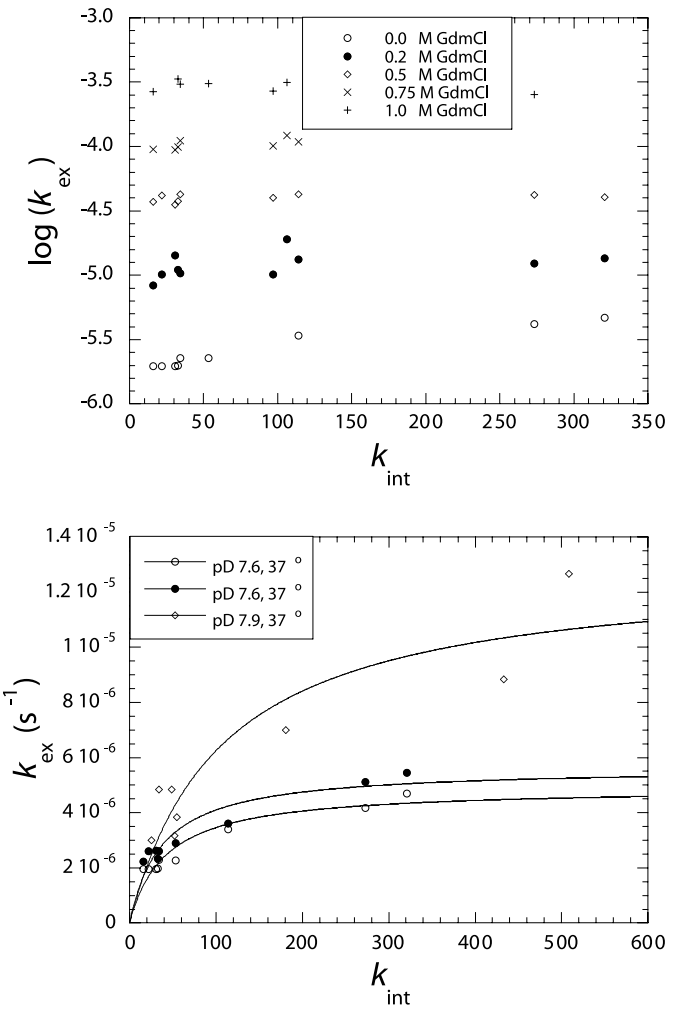

Figure 4. Plots of $\log k_{ex}$ *versus* k_{int} of mutant 43–80 under varying concentrations of GdmCl and plots of k_{ex} *versus* k_{int} at conditions indicated in the Figure. The continuous lines are fitted to the equation: $k_{ex} = k_{int}k_o(k_{int} + k_c)$.

these proteins as well as the others (Figure 5). The discrepancy of a factor of two to three between the intrinsic rate constants for exchange for barnase and those for model compounds is not unreasonable and within the limits of the method, given that the kinetics was measured under different conditions and also residues in a protein are in a different environment from those in a small model peptide.

At 37 °C and pH 7.6, there was excellent agreement between the observed rate constants for folding and k_c for wild-type at all concentrations of GdmCl examined (Figure 5), and for 85–102 and 43–80 above 0.5 M GdmCl. But, at very low concentrations of GdmCl, closing was faster than folding for 85–102, and some three times faster in ^2H_2O. There was also a marked discrepancy between the values for 43–80: closing was five times faster than folding at pH 7.7. As wild-type folded by effectively two-state kinetics under these conditions, it provided a good control. Thus, at pH 7.6 and 37 °C, 85–102 and 43–80 had closing rate constants that were higher than refolding rate constants, implying that the exchange-competent state had a higher refolding rate constant. These data are in agreement with the conclusions of Perrett *et al.* that 43–80 and 85–102 have closing rate constants that are higher than expected for a two-state mechanism (Table 3).

Equilibrium constants for denaturation of barnase

It is important to compare the free energy of unfolding obtained from hydrogen-exchange measurements with those from other procedures. Equilibrium denaturation was fitted to the standard equation. $\Delta G_{D-N} = \Delta G^{^2H_2O}_{D-N} - m_{D-N}[GdmCl]$, where ΔG_{D-N} is the free energy of the unfolding at a given concentration of GdmCl, $\Delta G^{^2H_2O}_{D-N}$ is the free energy of unfolding in ^2H_2O, and m_{D-N} is a constant. The equilibrium constants for denaturation were calculated using the data from equilibrium denaturation using GdmCl, stopped-flow data and hydrogen exchange experiments (Table 4). Equilibrium denaturation using a chemical denaturant is unreliable for accurate measurements, since the equations require extrapolation from a midpoint in higher concentrations of denaturant using an m_{D-N}-value that is very susceptible to experimental error and the assumption that the free energy of denaturation changes linearly with denaturant concentration. Experience is

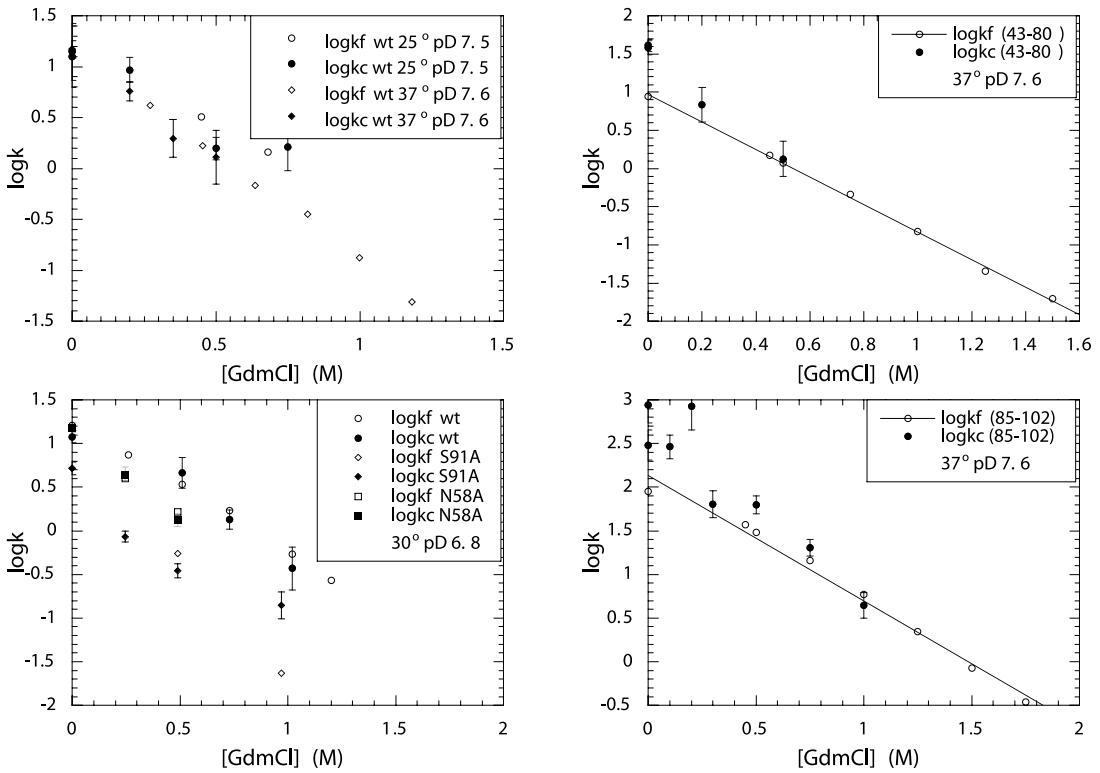

Figure 5. Plots of log k_c and log k_f *versus* GdmCl concentration for wild-type barnase (wt) and mutants 43–80, S91A, N58A and 85–102 at conditions indicated in the Figure. The continuous lines are the least squares fits through the values of log k_f.

that GdmCl denaturation can underestimate free energies of denaturation by 10–20%[33] but that differences in $\Delta G^{^2H_2O}_{D-N}$ between mutants can be measured accurately from the differences in $[GdmCl]_{50\%}$, the concentration of GdmCl at the midpoint. A possibly more accurate procedure is extrapolating the kinetic constants derived from chevron plots around the midpoint of denaturation assuming a two-state transition in this region, since intermediates are often kinetically silent around $[GdmCl]_{50\%}$. The most reliable procedure if a protein unfolds truly reversibly with temperature, as does wild-type barnase, is differential scanning calorimetry.[26,34]

The last column of Table 4 shows values of $\Delta\Delta G^{^2H_2O}_{D-N}$ calculated from $^1H/^2H$-exchange experiments using $\Delta G^{^2H_2O}_{D-N} = -RT \ln(k_o/k_c)$ and values of k_o and k_c that were either directly measured in

Table 4. Equilibrium constants for denaturation measured at equilibrium and by kinetics

Protein	Experimental conditions (°C, pH)	k_f/k_o[a]	k_c/k_o[a]	$\Delta\Delta G^{^2H_2O}_{D-N}$ Equilibrium (kcal mol^{-1})[b]	$\Delta\Delta G^{^2H_2O}_{D-N}$ ($RT \ln k_f/k_o$) (kcal mol^{-1})	$\Delta\Delta G^{^2H_2O}_{D-N}$ ($RT \ln k_c/k_o$) (kcal mol^{-1})
Wild-type	25, p^{2}H 7.5	$1.9(\pm0.3)\times10^8$	$1.8(\pm0.5)\times10^8$			
			$1.9(\pm0.9)\times10^7$			
	30, p^{2}H 6.8	$2.1(\pm0.3)\times10^7$	$2.1(\pm0.4)\times10^5$			
	37, p^{2}H 7.6	$2.1(\pm0.2)\times10^5$				
	37, p^{2}H 7.9	$6.1(\pm0.6)\times10^4$				
43-80	25, p^{2}H 7.5	$1.8(\pm0.1)\times10^6$	$6.6(\pm1.2)\times10^6$	$1.9(\pm0.1)$	$1.3(\pm0.07)$	$2.1(\pm0.15)$
	37, p^{2}H 7.6			$1.9(\pm0.1)$		
	37, p^{2}H 7.9			$1.8(\pm0.1)$		
85-102	25, p^{2}H 7.5	$2.4(\pm0.4)\times10^7$	$6.6(\pm1.8)\times10^7$	$4.3(\pm0.1)$	$2.9(\pm0.1)$	$3.5(\pm0.2)$
	37, p^{2}H 7.6			$4.6(\pm0.1)$		
	37, p^{2}H 7.9			$4.5(\pm0.1)$		
S91A	30, p^{2}H 6.8	$1.0(\pm0.1)\times10^6$	$4.1(\pm2.2)\times10^5$	$-1.8(\pm0.1)$	$-1.8(\pm0.09)$	$-2.3(\pm0.4)$
N58A	30, p^{2}H 6.8	$7.8(\pm0.6)\times10^5$	$8.4(\pm0.3)\times10^5$	$-1.8(\pm0.1)$	$-1.98(\pm0.08)$	$-1.9(\pm0.3)$

[a] Calculated from plots of log k_f, log k_c and log k_o *versus* [GdmCl].
[b] Calculated using average *m*-value of 4.91 kcal mol^{-1} M^{-1}. The standard errors were calculating by combining the errors for the individual rate and equilibrium constants as described.[1]

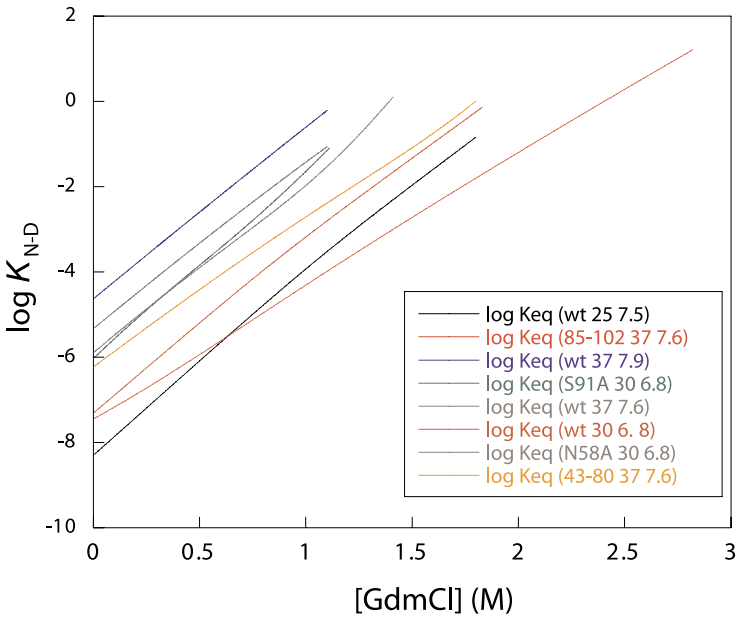

Figure 6. Plots of log K_{N-D} *versus* GdmCl concentration for wild-type barnase (wt) and mutants 43–80, S91A, N58A and 85–102 at conditions indicated in the Figure.

water or, where data were available, from the intercepts at 0 M GdmCl of plots of log k_o and log k_c *versus* [GdmCl]. These may be compared with values of $\Delta\Delta G^{^2H_2O}_{D-N}$ calculated from equivalent data from $\Delta G^{^2H_2O}_{D-N} = -RT \ln(k_o/k_f)$, where k_0 is the unfolding rate constant in water from the intercepts at 0 M GdmCl of plots of log k_f *versus* [GdmCl] for the three-state systems, or with $RT \ln(k_u/k_f)$ for the two-state systems, where k_u and k_f are the rate constants for unfolding and folding in water from the global fitting of the data in the chevron plots. There was excellent agreement between the values from kinetics, from exchange and from DSC for all the experiments with wild-type data and for the mutants N58A and S91A. But, for 43–80 and 85–102, the values from $^1H/^2H$-exchange were significantly higher than those calculated from kinetics, as expected from their closing rate constants being significantly higher than their observed folding rate constants. The exchange measurements agreed better with equilibrium measurements.

Positions of the transition states on the reaction pathway

We determined the position of the transition state on the reaction coordinate, in terms of solvent-accessible surface area, from the Tanford β-values (β_T), $\partial[\log k_u]/\partial[\text{GdmCl}])/(\partial \log K_{D-N}/\partial[\text{GdmCl}])$ at low concentrations of GdmCl. The slope of log k_u (where k_u is in most cases the value of k_o from exchange experiments) was calculated from the theoretical fits to the plots in Figures 1 and 3. K_{D-N} was calculated from the ratios of the values of k_u from those theoretical fits and the interpolated values of k_f under the same conditions (Figure 6).

The logarithms of k_o/k_f over the measured ranges (Figure 6) were reasonably linear in all cases and parallel, apart from shallower slopes for 85–102 and 43–80. The particularly low slope for 85–102 implied that the equilibrium being measured from k_o/k_f was between the native state and a denatured state that was much more compact than those for wild-type and the destabilized mutants and did not unfold. We conclude from the lower slope and the observation that $k_c \gg k_f$ that the denatured state of 85–102 is a compact folding intermediate, and much more stable than U, consistent with NMR studies.[35] We restricted the range of [GdmCl] for each mutant to that for which values of k_f were directly measured. The calculated values of β_T do not rest on the assumption that k_u and k_f fit the models that were used to derive the theoretical curves: those theoretical curves simulated very accurately the variation of k_u and k_f with GdmCl concentration and so they provided just an appropriate procedure for interpolating values of k_u and k_f and their slopes.

For wild-type at 25 °C and pH 7.5, β_U (the β-value for unfolding) changed from 0.3 at high-[GdmCl] to 0.68 in water (Figure 7), consistent with a change in rate-determining transition state for unfolding from native-like to denatured-like with decreasing concentrations of GdmCl. Conversely, β_F (the β-value for folding), which is $1 - \beta_U$, increased from 0.32 in water to 0.7 at high-[GdmCl], corresponding to a change from an early transition state to a late transition state for folding with increasing denaturant concentration. There was similar behaviour under three-state conditions at 30 °C and p^2H 6.8, with β_F changing from 0.26 to 0.67 (Figure 7). Under two-state conditions at 37 °C and pH 7.6, there was a shallower change in β_F from 0.51 to 0.66, and under the more extreme two-state conditions at 37 °C and pH 7.9, from 0.59 to a limiting value of 0.67. We fitted the β_F

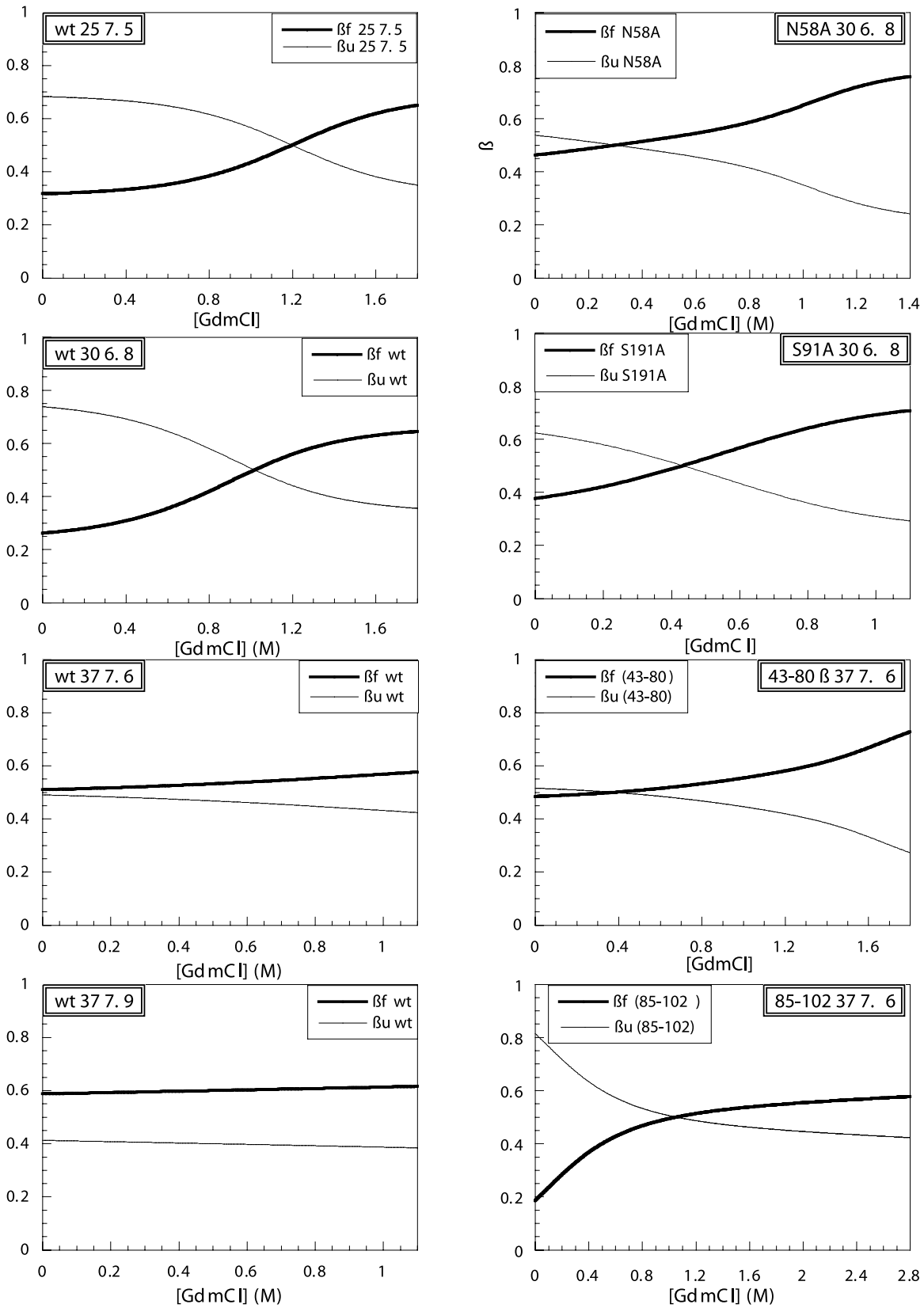

Figure 7. Tanford β-value for the folding and unfolding of wild-type barnase (wt) and mutants N58A, S91A, 43–80 and 85–102 at conditions indicated in the Figure.

values for wild-type at 25 °C and 30 °C to the theoretical curves for the equation $k_f = k_1k_2/(k_{-1} + k_2)$, assuming a linear dependence of the logarithm of each rate constant on GdmCl. The theoretical and experimental curves were superimposable, demonstrating that there is a switch from one rate determining transition state to another, and that there is not a general drift in transition state structure. Sanchez & Kiefhaber[7] have distinguished between general drifts and true changes in rate determining steps by a similar quantitative analysis of curvature in chevron plots.

The observed values of β_F for N58A in water was 0.47, rising to >0.7. The values for S91A were 0.38 and >0.7. 43–80 at 37 °C and pH 7.6 behaved like wild-type under the same conditions (Figure 7), with β_F increasing from 0.4 to 0.8. But β_F for 85–102 increased from 0.19 to 0.6 under the same conditions.

Discussion

Controls

There are inherent problems in analysing the kinetics and equilibria of protein folding in the presence of denaturant. To a first approximation, the free energy of denaturation of many proteins varies linearly with the concentration of either GdmCl or urea as do the logarithms of the rate constants of unfolding and refolding.[36,37] For many purposes, the linearity approximation can vary from being excellent to adequate. But, on closer inspection, there is curvature in the plots for equilibrium unfolding for barnase in urea solutions[33] and in the rate constants for unfolding[26] as well as in the refolding reactions.[2] GdmCl has its additional problems at low concentrations because it is ionic, and the changes in ionic strength may cause electrostatic interactions to change.[38] The electrostatic effects may be especially important in the denatured state of barnase because we know that there are electrostatic interactions that are important at low ionic strength that may be of importance in maintaining the structure of the fluid denatured state ensemble.[39] Because of these complexities, it is important to perform a variety of controls by varying the reaction conditions and, more importantly, by studying a range of mutants that have subtle variations in their structure. Comparative studies then may reveal the substantial facts beyond the complexities. Unfolding kinetics should be more reliable than refolding kinetics, since the starting point for unfolding is the native structure, which is the most robust on the folding pathway and hence the least susceptible to reaction conditions. The unfolding transition state should be the next most robust as it is more tightly packed than the early transition states in folding. Conversely, refolding kinetics is the least reliable as the poorly packed intermediates may be very susceptible to changes in environment. In the following analysis, we attempt to find general conclusions that are beyond the level of artifacts.

Proof of an unfolding intermediate

We measured the unfolding of barnase in the absence or at low concentrations of GdmCl by $^1H/^2H$-exchange kinetics and at high concentrations of GdmCl by conventional stopped-flow methods.[9] The dependence of the kinetics of unfolding of wild-type barnase on the concentration of denaturant showed clearly that there was an unfolding intermediate under conditions where barnase was previously postulated to fold by multi-state kinetics. The dependence of the logarithm of the unfolding rate constant on [GdmCl] fitted quantitatively to a three-state equation with a clear change in rate determining step (Figure 3). Under three-state conditions, the Tanford β-value, which is one measure of the position of the transition state on the reaction pathway, had a well-defined sigmoid transition with increasing concentrations of GdmCl that was consistent with a switch from one rate-determining step to another (Figure 7). It could, perhaps, be argued that there may be unknown artifacts that cause such sigmoid characteristics in plots against [GdmCl]. We eliminated the intrusion of artifacts by the two types of control experiments. Controls with wild-type protein were to change the reaction conditions to those that were known to favour (apparent) two-state folding by varying temperature and pH: at 37 °C and pH 7.5 or 7.9, there were just smooth, weak dependencies of both the unfolding rate constants and Tanford β-values on [GdmCl] (Figure 7). Controls under identical conditions to those where there were sigmoid changes for wild-type were made by studying the unfolding of two mutants (S91A and N58A) which are known to deviate less than wild-type from three-state kinetics. The unfolding of S91A and N58A showed relatively shallow changes in the dependence of their unfolding kinetics on [GdmCl] (Figure 3). Consistent data were also found for the two disulphide-linked mutants 43–80 and 85–102 (Figure 3). There is, beyond reasonable doubt, an intermediate in the unfolding of barnase.

Proof of a folding intermediate

The next argument is whether the unfolding pathway of barnase is the same as its folding pathway. The identity can be checked by comparing the measured free energy of denaturation at equilibrium with that calculated from the ratios of the observed rate constants for unfolding and refolding. We measured the rate constants for folding and unfolding well into the transition region of GdmCl-mediated denaturation by a combination of stopped-flow and $^1H/^2H$-exchange kinetics. The ratio of the rate constants for folding and unfolding or opening and closing of wild-type protein at 37 °C both gave, within experimental error, the

same free energy of denaturation in water (10.1 kcal/mol) as measured by thermal denaturation at equilibrium (10.4 kcal/mol) as previously reported.[9] Accordingly, there is, beyond reasonable doubt, an intermediate on the folding pathway of barnase.

Folding *versus* closing rate constants

As noted previously,[9] we believe that the rate constants for closing calculated from $^1H/^2H$-exchange using the web-based values are underestimates of the true values by a factor of 2.5 under our reaction conditions and for the protein environment of denatured barnase: using the conversion factor of 2.5, we found excellent agreement between the measured values of k_f and k_c for wild-type and for NA58 and SA191 under all conditions (Figure 5). k_c cannot be less than k_f and so an upward conversion factor is necessary. But, for 43–80 and 85–102, the measured values of k_c were much higher than those for k_f at p^2H 7.6 and 7.9 at 37 °C as [GdmCl] tended to zero (Figure 5). These data are consistent with the earlier observations of Perrett *et al.*, based on the retention of an EX1 mechanism at high pH values, that 43–80 and 85–102 must have closing rate constants that are higher than the observed folding rate constants and so there has to be an intermediate on the pathway. Further, calculations of the equilibrium constant for the denaturation of 85–102 and 43–80 based on the ratio of k_f and k_o underestimated the equilibrium values whereas those calculated from k_c and k_o were more realistic (Table 4).

It must be noted that the opening rate constants that are measured from exchange are independent of the tabulated values of k_{imt} and are equal to the limiting value of exchange rate constant at the EX1 limit. The proof of the unfolding intermediate from the kinks in the plots of unfolding rate constants is thus unaffected by the choice of k_{int}, and a discrepancy of a factor of two to three in k_c would not materially affect the arguments.

How many intermediates? The nature of the denatured state

The original presentation of the folding of barnase[3] proposed that there was at least one intermediate, with the possibility of more. There were subsequent indications for some mutants that there is more than one intermediate.[25] Sanchez & Kiefhaber fit chevron plots for the folding of barnase in urea solutions to the equations for two intermediates.[7] MD simulations also detect a second intermediate.[40] We also know from both experiment and simulation that the starting state for refolding is collapsed, with some native-like interactions.[35] Direct studies of denatured states of barnase under denaturing conditions by NMR detect residual helical structure and also the β-hairpin (residues around 86–99).[19,35] The peptide corresponding to the β-hairpin is also structured at even high concentrations (6 M) of urea.[21] Simulations in water reveal a denatured state with native-like topology and the first α-helix stabilized by contacts with other residues.[35,41] The NMR experiments show that the acid denatured state is more structured than the chemically denatured state. The denatured state has, therefore, a degree of structure under all experimentally observable conditions. Stopped-flow circular dichroism experiments[42] show that the denatured state under folding conditions is closer to the native structure (signal at 237 nm) than the acid or urea-denatured state. Accordingly, the denatured state of the protein under physiological conditions (D_{phys}), is a folding intermediate, I. It is possible that D_{phys} slides towards the fully unfolded state (U) with increasingly denaturing conditions in a second-order transition.[43]

We have now directly detected rapid structural changes in the denatured state using sub-ms continuous flow fluorimetry[30] (Figure 2). The acid-denatured state rearranges with a rate constant of 8000 s^{-1} in refolding buffer at pH 7.5, and the GdmCl-denatured state may well rearrange with a consistent rate constant on being jumped from 2.5 M GdmCl to 0.23 M, but this change is at the limit of detection. Unfortunately, the amplitudes of these changes are too small for a reliable systematic analysis, but they do show that the changes in structure observed by spectroscopy in the denatured state under different conditions do interconvert on a time-scale associated with intermediates in the early stages of folding.

Experiments that were conducted some 14 years ago using NMR to monitor $^1H/^2H$-exchange in pulsed labelling experiments to detect such an intermediate, required very high concentrations of protein. Under such conditions, many of the >NH groups in the intermediate were protected against exchange with solvent faster than the overall folding.[44,45] But, recent experiments using more modern methods and lower protein concentrations find that there is not detectable rapid protection.[10,11] The folding intermediate of barnase is known to dimerize at high concentrations[46] and so it is likely that the intermediate was stabilized in the earlier experiments. We must now assume, therefore, that the state D_{phys} (= I) is not well protected against $^1H/^2H$-exchange and so exchange can take place from D_{phys} and that it is not necessary to unfold to the fully unfolded state U for exchange. Accordingly, the existence of a change in rate determining step in unfolding with changing [GdmCl] as monitored by exchange implies that there must be an intermediate between D_{phys} (= I) and N (Figure 8).

The existence of an additional intermediate accounts for difference in behaviour of k_c and k_f between 43–80 and 85–102 and the other proteins. For wild-type and the non-cross-linked mutants, closing and folding are the same reaction. But, for the cross-linked mutants, the additional constraints on the structure of D_{phys} (see above and

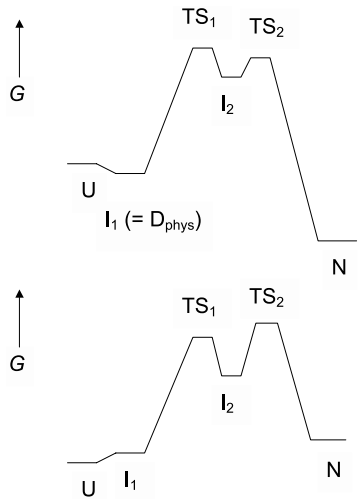

Figure 8. Minimal four-state folding pathway of barnase. Top, situation for wild-type barnase and similar mutants in the absence of denaturant and conditions that favour folding. Bottom, in the presence of concentrations of denaturant that favour unfolding. I_1 is a folding intermediate that is the denatured state under physiological conditions (D_{phys}). It is known from NMR and other spectroscopic experiments and simulation that D_{phys} is partly structured.

Clarke *et al.*[47]) means that it is partly protected against exchange and so exchange from U is also important.

Implications for refolding kinetics

The existence of two intermediates, one of which accumulates at low concentrations of denaturant, makes it difficult to analyse the kinetics of folding. The intermediates cause curvature in the refolding reaction by two effects: the change in population of D_{phys} and the change in partitioning with increasing [GdmCl]. Accordingly, there need not be the same partitioning ratios found in unfolding kinetics. Previously, the early folding intermediates were all assumed to be low-energy relative to U and they were lumped together so that the refolding rate constant was thought to report back on the average properties of all the sequential intermediates.[3,25] The refolding rate constant still reports back on the properties of the equilibrium mixture between U and D_{phys}.

The presence of the high-energy intermediate does affect the previous calculation of the equilibrium constant between U and D_{phys}. There is a large discrepancy between the equilibrium constant for denaturation measured at equilibrium and that calculated from the ratio of the observed refolding rate constant and the unfolding rate constant obtained from extrapolation of high denaturant to water. This was interpreted as the equilibrium constant between U and D_{phys}.[3,25] It is now clear from the present study, that a major contribution to the discrepancy is the partitioning ratio k_{-1}/k_2. It is also not easy to estimate the stability of D_{phys} relative to U in Figure 8. The equilibrium measurements of unfolding measure the transition between N and a mixture of D_{phys} and U, and the ratio of kinetic measurements report back on similar events, if not the same, interconversion. We just know that the observed D_{phys} is structured and accordingly the observed denatured state is of lower energy than U, but we do not know the relative free energies of the two.

Implications for Φ-value analysis

The Φ-value analysis[16,25,48] of the final transition state (I_2 to N) for the folding of barnase is unaffected by the new findings. The analysis of the structure of the intermediate I_2 is not materially affected. Importantly, we are now able to analyse the refolding data, since we now know that k_f represents the process of D_{phys} (i.e. I_1) going to I_2 and map the transition state (unpublished results).

Interpretation of Tanford β_F values

The Tanford β_F values have to be interpreted according to Figure 8. The β_F for the final transition state for folding is 0.7, based on the observed values for wild-type at pH 7.9 and 37 °C, which folds by close-to two state kinetics, and the limiting values for wild-type and other mutants at higher concentrations of GdmCl, where the kinetics switch to two state. The β_F value for the transition from I_1 to TS_1 for folding is 0.3, based on the limiting values for wild-type at 25 °C and 30 °C. We also conclude that the value of β_F for 85–102 of 0.2 in water is for the process of the intermediate going to the final transition state. This implies that the intermediate I_2 has a β_F of 0.7–0.2, i.e. 0.5.

Conclusions

There are two intermediates on the folding pathway of barnase. The first, I_1, is a loosely structured state of native-like topology, which is also the denatured state under physiological conditions, D_{phys} (U is of higher energy). This has not been proven to be on-pathway, but molecular dynamics simulation of unfolding[35,47,49] has this state formed from the native structure without prior complete unfolding and partial refolding, so that it is on pathway. The native-like topology of the first intermediate is the reason for the low Φ-values for the folding kinetics.[25] The second intermediate, I_2, is high energy. For wild-type barnase and most mutants, the rate-determining step in their folding in water is the formation of the second intermediate from D_{phys}. At moderate to high concentrations of denaturant, the kinetics switch to two-state because the energy of the second-transition state becomes higher and there is a single rate determining transition state. The same is true for increasing temperature. This high-energy state was proven here to be on-pathway.

Materials and Methods

Materials

$^{15}NH_4Cl$ and deuterated imidazole were obtained from Sigma; deuterium oxide was purchased from Goss chemicals Ltd. High-purity guanidine hydrochloride and ampicillin were obtained from Melford laboratories Ltd. Precast SDS-PAGE phastgels and molecular weight markers were from Amersham Pharmacia Biotech. SP-Trisacryl resin was purchased from BioSepra Life Technologies. Most other chemicals were from Sigma or BDH. The buffers used in equilibrium denaturation and stopped-flow experiments were 50 mM imidazole in ^2H_2O (p^2H 7.5, 7.6 and 7.9) and 50 mM Tris in ^2H_2O (p^2H 7.9) at 25 °C and 37 °C.

Methods

Expression and purification of mutant proteins

The pTZ416 vectors (adapted from pTZ18U)[50] harbouring wild-type and mutants S91A, N58A, 43–80 (A43C + S80C) and 85–102 (S85C + H102C) barnase gene were transformed into *Escherichia coli* C41 bacterial strain and used to express and purify barnase. The method of expression and purification have been described previously.[51] To produce uniformly ^{15}N-labelled proteins, the same strain was grown in minimal medium containing $^{15}NH_4Cl$ (0.5 mg/ml) as the sole nitrogen source. Proteins used in NMR experiments were found by SDS-PAGE to be >95% pure upon elution from Trisacryl ion-exchange resin and so were not purified further while the unlabelled proteins were further purified by FPLC, as described.

Fluorescence measurements

Measurements were made using an Aminco Bowman series 2 luminescence spectrophotometer and a Hitachi F4500 spectrofluorimeter. Filtered samples were placed in a 1 ml quartz Hellma cuvette maintained at 25 °C or 37 °C (measured by Edale Instruments thermocouple) using a Grant LTD20 circulation water bath. A stock solution of protein was made with concentration 30 μM in 50 mM imidazole buffer in ^2H_2O (p^2H 7.5 and 7.6) or in 50 mM Tris (p^2H 7.9). The Trp was excited at 280 nm using a 4 nm bandwidth. Emission spectra were obtained between 300–450 nm. An average of two scans at 1.5 nm s^{-1} was recorded.

Equilibrium denaturation experiments

Measurements were made using a Aminco Bowman spectrofluorimeter with a 1 cm path length cuvette at 25 °C and 37 °C. Buffered stock solutions of GdmCl were prepared (0 M and 8 M). After filtering the buffered stock, solutions were mixed in appropriate proportions to give final denaturant concentration ranging from 0 M to 5 M GdmCl (0.1 and 0.2 M increments) with a final protein concentration of 1 μM. All solutions were mixed by vortexing and equilibrated at 25 °C or 37 °C for about 12 hours.

Kinetic experiments

Kinetic unfolding and refolding measurements were performed using an Applied Photophysics SX.18MV stopped-flow fluorimeter. The temperature at the observation cell was regulated to 25 °C or 37 °C using a Grant LTD 6G water bath. Excitation was at 280 nm using a 2 mm excitation slit width (10 nm band width). A glass band-pass filter was used to measure emitted light above 320 nm or in some cases 360 nm from a cuvette of 2 mm path length. One thousand data points were acquired per reaction using log sampling and between 12–16 traces obtained at each denaturant concentration. These traces were overlaid, averaged and then fitted to single or double exponential functions using the manufacturer software.

Stopped-flow measurements of unfolding

Unfolding experiments were initiated by rapidly diluting one volume of native protein (50 μM concentration) in 50 mM imidazole or Tris in ^2H_2O (p^2H 7.5, 7.6 or 7.9) with ten volume of concentrated denaturant containing 50 mM imidazole or Tris in ^2H_2O (p^2H 7.5, 7.6 or 7.9). The final concentrations of GdmCl were in the range of 2–6 M.

Stopped-flow measurements of refolding

Refolding experiments were performed by 1:10 dilution of unfolded protein (50 μM protein in concentrated GdmCl, 50 mM imidazole or Tris in ^2H_2O, p^2H 7.5, 7.6 or 7.9) into buffered solutions with final GdmCl concentration in the range 0.3–3 M denaturant. Alternatively, the protein (50 μM) was denatured in 32 mM HCl at a pH of 1.5 and the solution was used for kinetic studies within 20–30 minutes. The refolding buffer was 100 mM imidazole or Tris in ^2H_2O with 27.5 mM HCl. Refolding was initiated by dilutions of acid-denatured protein with a refolding buffer at 1:1 ratio resulting in a final p^2H of 7.5, 7.6 or 7.9 and 50 mM imidazole or Tris.

Continuous-flow measurements

Sub-millisecond mixing experiments were performed as described[52] using the equipment as essentially described by Shastry *et al*.[30] The quartz flow cuvette was illuminated at 280 nm by using a Hg/Xe light source and fluorescence intensity was collected using a 330(±25) nm band-pass filter. The dead-time of the instrument, calibrated by measuring the quenching of *N*-acetyl-tryptophanamide fluorescence by *N*-bromo succinimide,[53] was 75–100 μs. Refolding of 32 mM HCl denatured wild-type barnase to pH 7.5, was measured at a final concentration of 10 μM at 25 °C. The data were recorded within five to ten minutes of denaturing the protein.

Nuclear magnetic resonance experiments

Exchange buffer (p^2H 7.5, 7.6 or 7.9) was prepared using ^2H_2O and the p^2H was measured, and corrected using a glass electrode ($p^2H = pH^{read} + 0.4$). The exchange buffer used in the experiment was 50 mM imidazole adjusted to p^2H 7.5 and 7.6 or 50 mM Tris p^2H 7.9 with ^2HCl containing 0.05% (w/v) sodium azide to prevent bacterial contamination during the exchange experiments. The non-exchange buffer was the same as above except that it was prepared using 90% water and 10% ^2H_2O. For assignment 20 mg of ^{15}N-labelled wild-type barnase was dissolved in appropriate buffer containing 90% water and 10% ^2H_2O.

Lyophilised, uniformly ^{15}N labelled protein was dissolved in exchange buffer (final concentration approximately 3 mM), the pH was adjusted, the sample was then centrifuged to remove any insoluble protein and transferred to a NMR tube and into the magnet. The first spectrum was recorded approximately 20 minutes after the solution of the protein. The samples were maintained at 25 °C or 37 °C, in the NMR tube throughout the study. The final p^2H was measured using a glass electrode at the temperature of the experiment.

$^1H-^{15}N$ HSQC spectra[54] were acquired on a Bruker AMX500 spectrometer utilising 2000 complex data points over 4000 Hz in ^1H dimension and 256 increments over 3000 Hz in the ^{15}N dimension. The chemical shifts of the backbone amides were assigned by comparison with previously assigned spectra.[55] Each sample was shimmed and tuned before the start of data acquisition. The length of the 90° pulse was determined by adjusting the *p*1 value until the transformed and phased ^1H water peak showed equal areas above and below the baseline. ^{15}N HSQC spectra were acquired at regular intervals. In the first two hours, ten spectra were acquired (two scans per experiment), followed by six spectra in the next two hours (four scans per experiment) and thereafter spectra with total increment time of about 40 minutes (eight scans per experiment), were acquired at increasing intervals, ranging from one hour to several weeks. About 40 experiments were performed in the first 24 hours.

The first HSQC spectrum in each experiment was phased using the software NMRView[56] to obtain *p*0 and *p*1 values in each dimension. All subsequent spectra were phased by inputting these values into NMRPipe.[57] The volume integrals of the cross peaks were calculated by NMRView and plotted against time. The data were transferred to a Macintosh computer and the decays were fitted to a single exponential, using the program KaleidaGraph. Where the rate of exchange was very slow, and the decay could not be fitted to an exponential, but where an initial rate could be determined, a rate constant was calculated from the ratio of the slope (initial rate) to the estimated amplitude of decay.

Acknowledgements

S.G. is supported by a fellowship from the Istituto Pasteur-Fondazione Cenci Bolognetti (Rome, Italy). We thank Dr Jane Clarke for helpful advice.

References

1. Fersht, A. (1999). *Structure and Mechanism in Protein Science*, W. H. Freeman and Co., New York.
2. Matouschek, A., Kellis, J. T. J., Serrano, L. & Fersht, A. R. (1989). Mapping the transition state and pathway of protein folding by protein engineering. *Nature*, **340**, 122–126.
3. Matouschek, A., Kellis, J., Jr, Serrano, L., Bycroft, M. & Fersht, A. R. (1990). Transient folding intermediates characterized by protein engineering. *Nature*, **346**, 440–445.
4. Matouschek, A. & Fersht, A. R. (1991). Protein engineering in analysis of protein folding pathways and stability. *Methods Enzymol.* **202**, 82–112.
5. Krantz, B. A., Mayne, L., Rumbley, J., Englander, S. W. & Sosnick, T. R. (2002). Fast and slow intermediate accumulation and the initial barrier mechanism in protein folding. *J. Mol. Biol.* **324**, 359–371.
6. Jackson, S. E. & Fersht, A. R. (1991). Folding of chymotrypsin inhibitor 2.1. Evidence for a two-state transition. *Biochemistry*, **30**, 10428–10435.
7. Sanchez, I. E. & Kiefhaber, T. (2003). Hammond behaviour *versus* ground state effects in protein folding: evidence for narrow free energy barriers and residual structure in unfolded states. *J. Mol. Biol.* **327**, 867–884.
8. Sanchez, I. E. & Kiefhaber, T. (2002). Evidence for sequential barriers and obligatory intermediates in apparent two-state protein folding. *J. Mol. Biol.* **325**, 367–376.
9. Fersht, A. R. (2000). A kinetically significant intermediate in the folding of barnase. *Proc. Natl Acad. Sci. USA*, **97**, 14121–14126.
10. Takei, J., Chu, R.-A. & Bai, Y. (2000). Absence of stable intermediates on the folding pathway of barnase. *Proc. Natl Acad. Sci. USA*, **97**, 10796–10801.
11. Chu, R.-A., Takei, J., Barchi, J. J. & Bai, Y. (1999). Relationship between the native-state hydrogen exchange and the folding pathways of barnase. *Biochemistry*, **38**, 14119–14121.
12. Chu, R.-A. & Bai, Y. (2002). Lack of definable nucleation sites in the rate-limiting transition state of barnase under native conditions. *J. Mol. Biol.* **315**, 759–770.
13. Jonsson, T., Waldburger, C. D. & Sauer, R. T. (1996). Nonlinear free energy relationships in Arc repressor unfolding imply the existence of unstable. Native-like folding intermediates. *Biochemistry*, **35**, 4795–4802.
14. Kiefhaber, T., Bachmann, A., Wildegger, G. & Wagner, C. (1997). Direct measurement of nucleation and growth rates in lysozyme folding. *Biochemistry*, **36**, 5108–5112.
15. Walkenhorst, W. F., Green, S. M. & Roder, H. (1997). Kinetic evidence for folding and unfolding intermediates in Staphylococcal nuclease. *Biochemistry*, **36**, 5795–5805.
16. Serrano, L., Kellis, J., Cann, P., Matouschek, A. & Fersht, A. R. (1992). The folding of an enzyme. II. Substructure of barnase and the contribution of different interactions to protein stability. *J. Mol. Biol.* **224**, 783–804.
17. Clarke, J., Hounslow, A. M., Bycroft, M. & Fersht, A. R. (1993). Local breathing and global unfolding in hydrogen-exchange of barnase and its relationship to protein folding pathways. *Proc. Natl Acad. Sci. USA*, **90**, 9837–9841.
18. Perrett, S., Clarke, J., Hounslow, A. M. & Fersht, A. R. (1995). Relationship between equilibrium amide proton exchange behavior and the folding pathway of barnase. *Biochemistry*, **34**, 9288–9298.
19. Arcus, V. L., Vuilleumier, S., Freund, S. M., Bycroft, M. & Fersht, A. R. (1995). A comparison of the pH, urea, and temperature-denatured states of barnase by heteronuclear NMR: implications for the initiation of protein folding. *J. Mol. Biol.* **254**, 305–321.
20. Wong, K., Freund, S. M. V. & Fersht, A. R. (1996). Cold denaturation of barstar: ^1H,^{15}N and ^{13}C NMR assignment and characterisation of residual structure. *J. Mol. Biol.* **259**, 805–818.
21. Neira, J. L. & Fersht, A. R. (1996). An NMR study on

the beta-hairpin region of barnase. *Fold Des.* **1**, 231–241.
22. Clarke, J., Henrick, K. & Fersht, A. R. (1995). Disulfide mutants of barnase. I: Changes in stability and structure assessed by biophysical methods and X-ray crystallography. *J. Mol. Biol.* **253**, 493–504.
23. Clarke, J., Hounslow, A. M. & Fersht, A. R. (1995). Disulfide mutants of barnase. II: Changes in structure and local stability identified by hydrogen exchange. *J. Mol. Biol.* **253**, 505–513.
24. Li, A. & Daggett, V. (1998). Molecular dynamics simulation of the unfolding of barnase: charaterization of the major intermediate. *J. Mol. Biol.* **275**, 677–694.
25. Matouschek, A., Serrano, L. & Fersht, A. R. (1992). The folding of an enzyme. IV. Structure of an intermediate in the refolding of barnase analysed by a protein engineering procedure. *J. Mol. Biol.* **224**, 819–835.
26. Matouschek, A., Matthews, J. M., Johnson, C. M. & Fersht, A. R. (1994). Extrapolation to water of kinetic and equilibrium data for the unfolding of barnase in urea solutions. *Protein Eng.* **7**, 1089–1095.
27. Dalby, P. A., Oliveberg, M. & Fersht, A. R. (1998). Movement of the intermediate and rate determining transition state of barnase on the energy landscape with changing temperature. *Biochemistry*, **37**, 4674–4679.
28. Dalby, P. A., Oliveberg, M. & Fersht, A. R. (1998). Folding intermediates of wild-type and mutants of barnase. I. Use of phi-value analysis and *m*-values to probe the cooperative nature of the folding pre-equilibrium. *J. Mol. Biol.* **276**, 625–646.
29. Bachmann, A. & Kiefhaber, T. (2001). Apparent two-state tendamistat folding is a sequential process along a defined route. *J. Mol. Biol.* **306**, 375–386.
30. Shastry, M. C. R., Luck, S. D. & Roder, H. (1998). A continuous-flow capillary mixing method to monitor reactions on a microsecond time-scale. *Biophys. J.* **74**, 2714–2721.
31. Hvidt, A. A. & Nielsen, S. O. (1966). Hydrogen exchange in proteins. *Advan. Protein Chem.* **21**, 287–386.
32. Bai, Y., Milne, J. S., Mayne, L. & Englander, S. W. (1993). Primary structure effects on peptide group hydrogen exchange. *Proteins: Struct. Funct. Genet.* **17**, 75–86.
33. Johnson, C. M. & Fersht, A. R. (1995). Protein stability as a function of denaturant concentration: the thermal stability of barnase in the presence of urea. *Biochemistry*, **34**, 6795–6804.
34. Martinez, J. C., El Harrous, M., Filimonov, V. V., Mateo, P. L. & Fersht, A. R. (1994). A calorimetric study of the thermal stability of barnase and its interaction with 3′GMP. *Biochemistry*, **33**, 3926–3939.
35. Wong, K. B., Clarke, J., Bond, C. J., Neira, J. L., Freund, S. M., Fersht, A. R. & Daggett, V. (2000). Towards a complete description of the structural and dynamic properties of the denatured state of Barnase and the role of residual structure in folding. *J. Mol. Biol.* **296**, 1257–1282.
36. Tanford, C. (1968). Protein denaturation. *Advan. Protein. Chem.* **23**, 121–282.
37. Pace, C. N. (1986). Determination and analysis of urea and guanidinium hydrochloride denaturation curves. *Methods Enzymol.* **131**, 266–280.
38. Shortle, D., Meeker, A. K. & Freire, E. (1989). Effects of denaturants at low concentrations on the reversible denaturation of staphylococcal nuclease. *Arch. Biochem. Biophys.* **272**, 103–113.
39. Oliveberg, M., Vuilleumier, S. & Fersht, A. R. (1994). Thermodynamic study of the acid denaturation of barnase and its dependence on ionic strength: evidence for residual electrostatic interactions in the acid/thermally denatured state. *Biochemistry*, **33**, 8826–8832.
40. Li, A. J. & Daggett, V. (1998). Molecular dynamics simulation of the unfolding of barnase: characterization of the major intermediate. *J. Mol. Biol.* **275**, 677–694.
41. Daggett, V., Li, A. & Fersht, A. R. (1998). Combined molecular dynamics and phi value analysis of structure–reactivity relationships in the transition state and unfolding pathway of barnase: structural basis of Hammond and anti-Hammond effects. *J. Am. Chem. Soc.* **120**, 12740–12754.
42. Oliveberg, M. & Fersht, A. R. (1996). Thermodynamics of transient conformations in the folding pathway of Barnase: reorganization of the folding intermediate at low pH. *Biochemistry*, **35**, 2738–2749.
43. Dill, K. A. & Shortle, D. (1991). Denatured states of proteins. *Annu. Rev. Biochem.* **60**, 795–825.
44. Bycroft, M., Matouschek, A., Kellis, J., Jr, Serrano, L. & Fersht, A. R. (1990). Detection and characterization of a folding intermediate in barnase by NMR. *Nature*, **346**, 488–490.
45. Matouschek, A., Serrano, L., Meiering, E. M., Bycroft, M. & Fersht, A. R. (1992). The folding of an enzyme. V. H/^{2}H exchange-nuclear magnetic resonance studies on the folding pathway of barnase: complementarity to and agreement with protein engineering studies. *J. Mol. Biol.* **224**, 837–845.
46. Sanz, J. M., Johnson, C. M. & Fersht, A. R. (1994). The A-state of barnase. *Biochemistry*, **33**, 11189–11199.
47. Clarke, J., Hounslow, A. M., Bond, C. J., Fersht, A. R. & Daggett, V. (2000). The effects of disulphide bonds on the denatured state of barnase. *Protein Sci.* **9**, 2394–2404.
48. Serrano, L., Matouschek, A. & Fersht, A. R. (1992). The folding of an enzyme III. Structure of the transition state for unfolding of barnase analysed by protein engineering procedure. *J. Mol. Biol.* **224**, 805–818.
49. Bond, C. J., Wong, K. B., Clarke, J., Fersht, A. R. & Daggett, V. (1997). Characterization of residual structure in the thermally denatured state of barnase by simulation and experiment: description of the folding pathway. *Proc. Natl Acad. Sci. USA*, **94**, 13409–13413.
50. Hartley, R. W. (1988). Barnase and barstar. Expression of its cloned inhibitor permits expression of a cloned ribonuclease. *J. Mol. Biol.* **202**, 913–915.
51. Massakowska, D. E., Nyberg, K. & Fersht, A. R. (1989). Kinetic characterization of the recombinant ribonuclease from *Bacillus amyloliquefaciens* and investigation of key residues in catalysis by side-directed mutagenesis. *Biochemistry*, **28**, 3843–3850.
52. Ferguson, N., Johnson, C. M., Macias, M., Oschkinat, H. & Fersht, A. R. (2001). Ultrafast folding of WW domains without structured aromatic clusters in the denatured state. *Proc. Natl Acad. Sci. USA*, **98**, 13002–13007.
53. Peterman, B. F. (1979). Measurement of the dead-time of a fluorescence stopped-flow instrument. *Anal. Biochem.* **93**, 442–444.
54. Bax, A., Ikura, M., Kay, L. E., Torchia, D. A. & Tschudin, R. (1990). Comparison of different modes

of 2-dimensional reverse correlation NMR for the study of proteins. *J. Magn. Reson.* **86**, 304–318.
55. Jones, D. N. M., Bycroft, M., Lubienski, M. J. & Fersht, A. R. (1993). Identification of the barstar binding site of barnase by NMR spectroscopy and hydrogen–deuterium exchange. *FEBS Letters*, **331**, 165–171.
56. Johnson, B. A. & Blevins, R. A. (1994). NMRView—a computer programme for the visualization and analysis of NMR data. *J. Biomol. NMR*, **4**, 603–614.
57. Delaglio, F. (1995). NMRPipe: a multidimensional spectral processing system based on UNIX pipes. *J. Biomol. NMR*, **6**, 277–293.

Edited by C. R. Matthews

(Received 14 May 2003; received in revised form 7 August 2003; accepted 8 August 2003)